DYNAMIC PROPERTIES OF CLAY FOR EARTHQUAKE RESPONSE ANALYSIS IN THE BAY OF CAMPECHE

Víctor Manuel Taboada Urtuzuástegui[(1)], Shuang Cindy Cao[(2)], Diego Cruz Roque[(3)], Francisco Alonso Flores-López[(4)], Prócoro Barrera[(3)], Kuat C. Gan[(1)], Vishal Dantal[(5)], Esteban Ernesto Espinosa Samudio[(6)], Sergio Dionicio Renovato Carrión[(6)] y Juan Manuel Hernández Durón[(6)]

ABSTRACT

The Bay of Campeche is located in a region of moderate to high seismic activity related to the active triple junction between the North American, Caribbean, and Cocos plate boundaries. Therefore, the fixed offshore platforms and subsea structures in the Bay of Campeche must be designed against earthquake loading. A database was developed of classification and index properties tests, in situ measurements of shear wave velocity using downhole P-S suspension seismic velocity logging, in situ piezocone penetration tests, resonant column tests to characterize the shear modulus and material damping ratio at small shear strains (10^{-5} % to about 0.1 %), and strain-controlled cyclic direct simple shear tests to evaluate the decrease of shear modulus and the increase of material damping ratio at large shear strains (0.1 % to about 10 %) performed on clays from the Bay of Campeche, including clays with no carbonate content to 100 % carbonate content, retrieved from the seafloor to a penetration depth of 120 m below seafloor. The database was tailored specifically to develop empirical correlations for the Bay of Campeche clay to determine V_s when in situ measurements of V_s are not available and to develop numerical modeling to predict the variation of the normalized shear modulus (G/G_{max}) and material damping ratio as a function of shear strains (γ) when dynamic test results are unavailable for all the clay layers. The equations developed to calculate V_s and the curves of G/G_{max}-γ and D-γ of Bay of Campeche clays are recommended for preliminary or perhaps even final seismic site response evaluations.

Keywords: Bay of Campeche; earthquake response analysis; shear wave velocity; shear modulus; material damping ratio

ISSN-e 2395-8251

Artículo recibido el 09 de julio de 2021 y aprobado para su publicación el 29 de diciembre de 2022. Se aceptarán comentarios y/o discusiones hasta cinco meses después de su publicación.

(1) Fugro, 6100 Hillcroft Avenue, Houston, Texas 77081, USA, vtaboada@fugro.com, kgan@fugro.com
(2) Changzhou University, Department of Civil Engineering, Changzhou, Jiangsu Province, 213164, China, scaocindy@163.com
(3) Instituto Mexicano del Petróleo (IMP), Coordinación de Geotecnia Marina, Eje Central Lázaro Cárdenas Norte 152, San Bartolo Atepehuacan, Ciudad de México, México, C.P. 07730, dcruz@imp.mx, pbarrera@imp.mx
(4) Ingenieros Geotecnistas Mexicanos (IGM), Barbero de Sevilla Mza 7 Lt 4, Agrícola Metropolitana, Tláhuac, Ciudad de México, México C.P. 13280, alonso.fafl@igmmexico.com
(5) Norwegian Geotechnical Institute (NGI), PO Box 3930 Ullevaal Stadion, N-0806 Oslo, Norway, vishal.dantal@ngi.no
(6) PEMEX Exploración y Producción, Ciudad del Carmen, Campeche, México, sergio.dionicio.renovato@pemex.com, juan.manuel.hernandezd@pemex.com

DOI: 10.18867/ris.109.596

PROPIEDADES DINÁMICAS DE ARCILLA PARA EL ANÁLISIS DE RESPUESTA SÍSMICA EN LA BAHÍA DE CAMPECHE

RESUMEN

La Bahía de Campeche se encuentra en una región de moderada a alta actividad sísmica relacionada con la triple unión activa entre los límites de las placas de América del Norte, el Caribe y la de Cocos. Por lo tanto, las plataformas fijas en alta mar y las estructuras submarinas en la Bahía de Campeche deben diseñarse contra la carga sísmica. Una base de datos de pruebas de clasificación y propiedades índice, mediciones in situ de la velocidad de la onda de corte V_s utilizando la sonda suspendida, pruebas in situ de piezocono penetrómetro (PCPT), pruebas de columna resonante para caracterizar el módulo de rigidez y la relación de amortiguación del material a bajas deformaciones angulares (10^{-5} % a aproximadamente 0.1 %) y pruebas cíclicas de corte simple directo (DSS) con deformación controlada para evaluar la disminución del módulo de rigidez y el aumento de la relación de amortiguación del material a deformaciones angulares altas (0.1 % a aproximadamente 10 %) realizados en arcillas de la Bahía de Campeche incluyendo arcillas sin contenido de carbonato hasta el 100% del contenido de carbonato recuperados desde el fondo marino y hasta a una profundidad de 120 m por debajo del fondo marino. La base de datos fue diseñada específicamente para desarrollar para las arcillas de la Bahía de Campeche correlaciones empíricas para determinar V_s, cuando no se dispone de mediciones in situ de V_s, y modelos numéricos para predecir la variación del módulo de rigidez normalizado (G/G_{max}) y la relación de amortiguamiento de materiales en función de la deformación angular (γ) cuando no hay resultados de pruebas dinámicas disponibles para todas las capas de arcilla. Las ecuaciones desarrolladas para calcular V_s, y las curvas de G/G_{max}-γ y D-γ de las arcillas de la Bahía de Campeche se recomiendan para evaluaciones preliminares o tal vez incluso finales de respuesta sísmica del sitio.

Palabras Clave: Bahía de Campeche; análisis de respuesta sísmica; velocidad de onda de cortante; módulo de rigidez; relación de amortiguación del material

ISSN-e 2395-8251

INTRODUCTION

The Bay of Campeche is located in the large bay comprising the southern portion of the Gulf of Mexico between the Yucatan Peninsula to the east, the Isthmus of Tehuantepec to the south, and the coast of Mexico at Veracruz to the west. It is enclosed approximately by longitude 91° W on the east, longitude 94° W on the west, latitude 20° N on the north, and the Mexican coast on the south.

The Bay of Campeche is located in a region of moderate to high seismic activity related to the active triple junction between the North American, Caribbean, and Cocos plate boundaries. Therefore, the fixed offshore platforms and subsea structures in the Bay of Campeche must be design against earthquake loading. The most important soil dynamic properties to perform earthquake response analysis include shear wave velocity (V_s), shear modulus (G_{max}), material damping ratio (D_{min}) at low shear strains (less than 0.0001 %), and nonlinear shear modulus (G) and material damping ratio (D) as functions of shear strain (γ).

Unfortunately, an engineer responsible for performing earthquake response analysis in the Bay of Campeche sometimes does not have in situ measurements of shear wave velocity, and sometimes the dynamic testing performed with resonant column and strain-controlled cyclic direct simple shear (DSS) is limited and cannot be performed for all the clay layers found in the soil deposit. Therefore, the engineer has

to utilize semiempirical correlations to estimate the shear wave velocity, and the available normalized modulus reduction and damping ratio curves either are not based on marine clays or were developed for marine clays from a different geological setting with different soil characteristics from the Bay of Campeche clays.

Therefore, it was necessary to develop a database of classification and index properties tests, in situ measurements of shear wave velocity using downhole P-S suspension seismic velocity logging, in situ piezocone penetration tests (PCPTs), resonant column tests to characterize the shear modulus and material damping ratio at small shear strains (10^{-5} % to about 0.1 %), and strain-controlled cyclic DSS tests to evaluate the decrease of shear modulus and the increase of material damping ratio at large shear strains (0.1 % to about 10 %) performed on clay from the Bay of Campeche, including clays with no carbonate content to 100 % of carbonate content retrieved from the seafloor to a penetration depth of 120 m below seafloor (BSF). The database was tailored specifically to develop empirical correlations for the Bay of Campeche clays to determine V_s when in situ measurements of V_s are not available and to develop numerical modeling to predict the variation of the normalized shear modulus (G/G_{max}) and material damping ratio as a function of shear strains when no dynamic test results are available for all the clay layers.

The semiempirical correlations and the numerical modeling equations developed to determine the most important dynamic soil properties for earthquake response analysis of the marine clays of the Bay of Campeche are presented below.

ISSN-e 2395-8251

SHEAR WAVE VELOCITY OF BAY OF CAMPECHE CLAY

Summary of database of shear wave velocity of clay

A database with the results of the classification and index properties tests, in situ measurements of shear wave velocity every 0.5 m over the depth interval of 3.5 m to 121.9 m BSF using downhole P-S suspension seismic velocity logging, and in situ PCPTs for clay from 11 sites was assembled and tailored to develop semiempirical correlations to determine the shear wave velocity (Taboada, et al., 2013).

Figure 1 present histograms of some of the index and engineering properties included in the Bay of Campeche database of shear wave velocity. Natural water content (w) data range between 20 % and 90 % with most of the data in the range of 40 % to 60 %. The void ratio (e_o) data vary between 0.6 and 2.4 with the majority of the values in the range of 1.0 to 1.6. The liquid limit (W_L) varies between 40 % and 140 % with most of the values falling in the narrow band between 70 % and 90 %. The plastic index (Ip) data is defined as the difference between the liquid and plastic limits and varies between 50 % and 60 %. The effective vertical stress in the database varies between 17 kPa and 1100 kPa with the highest number of observations at around 200 kPa, corresponding to a depth of approximately 30 m BSF. The overconsolidation ratio (OCR) data range between 1.0 and 7.5 with most of the OCR data falling between 1.5 and 2.5, indicating most of the soil samples in the database are normally consolidated to lightly over consolidated clays. The shear strength data are concentrated in two groups: The first group of shear strength data range between 10 kPa and 40 kPa, with most of the data between 20 kPa and 30 kPa, representing the clays near the seafloor. In general, these clays are normally consolidated. The second group of shear strength data between 50 kPa to 450 kPa occurs in deeper strata. Most of the shear strength data in the second group range between 100 kPa and 300 kPa. The net cone resistance of the database falls within a wide range of 0.5 MPa to 7.5 MPa, with the highest number of observations at 0.5 MPa, which corresponds to a shallow depth of about 5 m to 10 m BSF. The in situ shear wave velocity (V_S) data range between 100 m/s and 550 m/s with the majority of the data between 150 m/s and 400 m/s.

ISSN-e 2395-8251

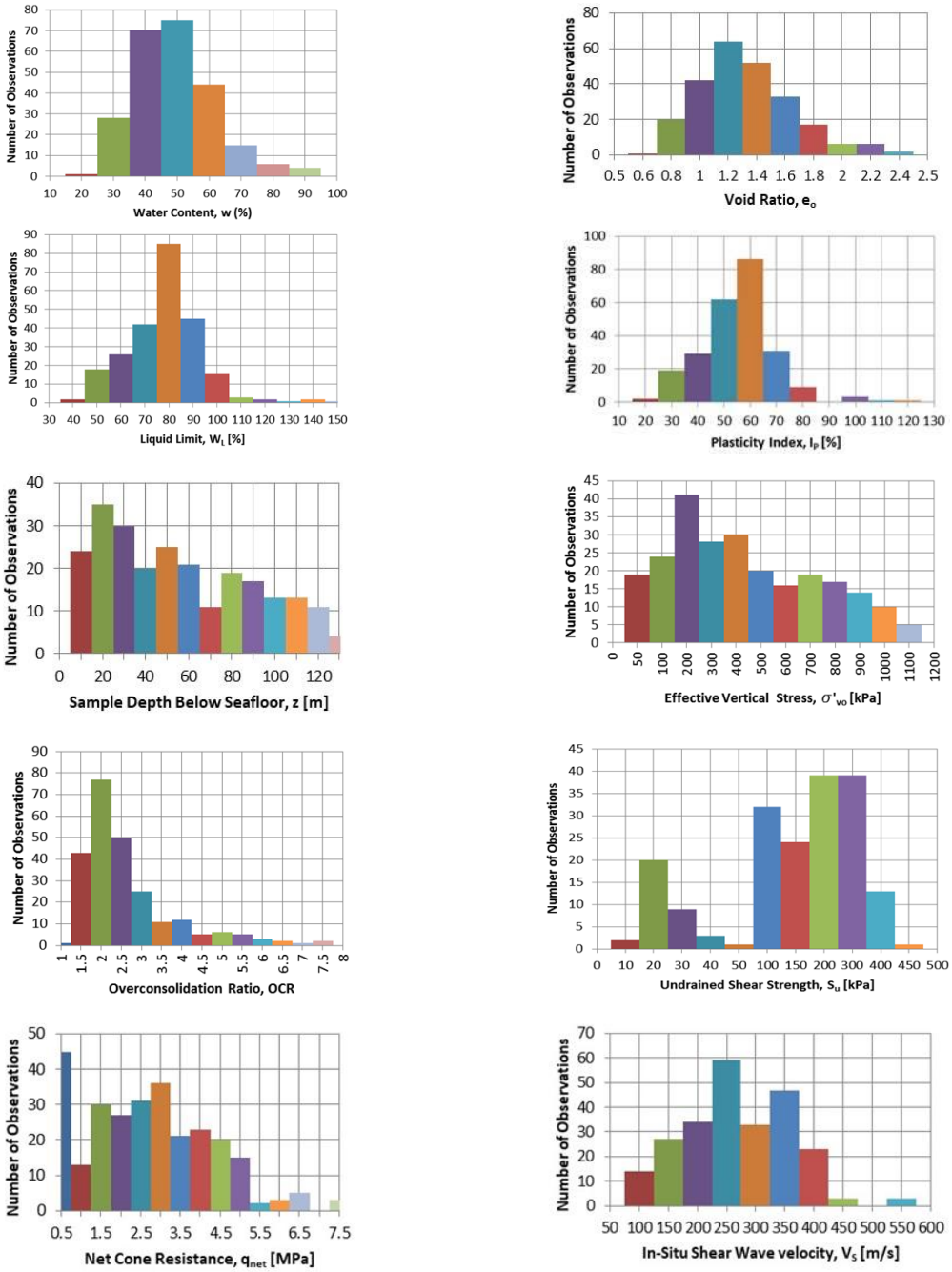

Figure 1. Histograms of the database of shear wave velocity of clays

Figure 2 presents the Casagrande plasticity chart with all the data from the 11 sites in the database numbered from S1 to S11. The data show a wide range of values with most of the data plotting in a fairly tight band above the A-line and the liquid limit greater than 50 % indicating predominantly high-plasticity clay type of soils.

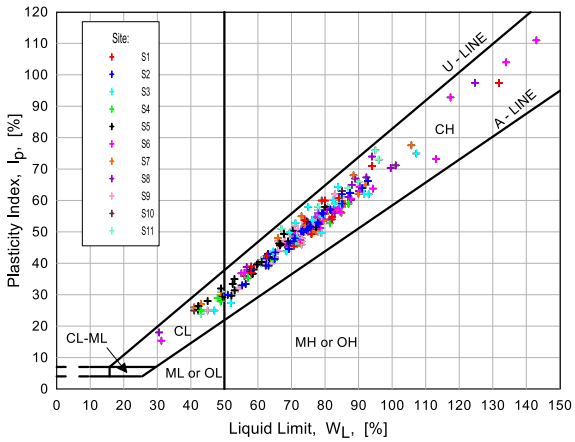

Figure 2. Plasticity chart with data from the 11 sites (S1 to S11) of the Bay of Campeche clay database

Multiple regression analyses for shear wave velocity of clay

The direct measurement of the in-situ shear wave velocity provides the most reliable and certain means of obtaining the shear modulus at low shear strains (less than 10^{-4} %) G_{max}. It can be calculated as a function of total mass density (ρ_{tot}) and shear wave velocity as:

$$G_{max} = \rho_{tot} V_S^2 \quad (1)$$

where $\rho_{tot} = \gamma_{tot}/g$, γ_{tot} = total unit weight, and g = gravitational acceleration constant = 9.80 m/s^2. Since the total mass density can be estimated with reasonable accuracy, the shear wave velocity or shear modulus at low shear strains can essentially be used interchangeably.

Multiple regression analyses were conducted in log-log format to provide power function expressions for V_S in terms of several variables. This section presents a summary of the most prominent correlations derived using multiple regression analyses.

The relationship with the highest coefficient of correlation using three variables was:

$$V_S = 26 S_u^{0.184} \left(\frac{\sigma'_{vo}}{w}\right)^{0.195} \quad (2)$$

where s_u (undrained shear strength) and σ'_{vo} (effective vertical stress) are in kPa, water content (w) is in decimal form, and V_S is in m/s. The coefficient of determination (r^2) is 0.951, and a total of 183 datasets (V_S, s_u, σ'_{vo}, and w) were used in the multiple regression analyses. This equation is recommended to estimate the in situ V_S due to its high coefficient of correlation and simplicity and due to the fact that when the overconsolidation ratio was further added, no improvement in the correlation was attained.

The expression with the highest correlation derived without involving the undrained shear strength and the net cone resistance was:

$$V_S = \frac{26(\sigma'_{vo})^{0.368} OCR^{0.174}}{e_o^{0.204}} \quad (3)$$

ISSN-e 2395-8251

where V_S is in m/s and σ'_{vo} is in kPa. The void ratio is defined as e_o and the overconsolidation ratio as OCR. The coefficient of determination is 0.925, and a total of 243 datasets were used in the analyses.

Multiple regression analyses also were conducted to provide power function expressions for in situ V_S in terms of cone net resistance (q_{net}) obtained from PCPTs and of soil properties. The expression with the highest correlation using the net cone resistance and two additional variables was:

$$V_S = 16.3(q_{net})^{0.209}(\frac{\sigma'_{vo}}{w})^{0.165} \quad (4)$$

where q_{net} and σ'_{vo} are in kPa, water content (w) is in decimal form, and V_S is in m/s. The coefficient of determination is 0.948 and a total of 274 datasets were used in the analyses.

Application of the most prominent empirical correlations to determine V_S in clay

A comparison between measured and predicted V_S profiles using the three equations with the highest correlation, equations (2), (3), and (4), is presented in figure 3 for a blind prediction (site not included in the database). Profiles of effective vertical stress (σ'_{vo}), water content (w), void ratio (e_o), and stress history (OCR) were developed for each site to generate the predicted V_S profiles presented in figure 3. A roman numeral representing each stratum is shown in figure 3.

ISSN-e 2395-8251

Figure 3 presents predicted and measured V_S profiles for the blind prediction, a soil deposit highly stratified with five very soft to hard calcareous clay layers interbedded with four layers of dense to very dense siliceous carbonate silty sand. There is a very good agreement between measured and predicted V_S in clay despite the fact that at the site the clay strata are interbedded with relative thick layers of silty sand.

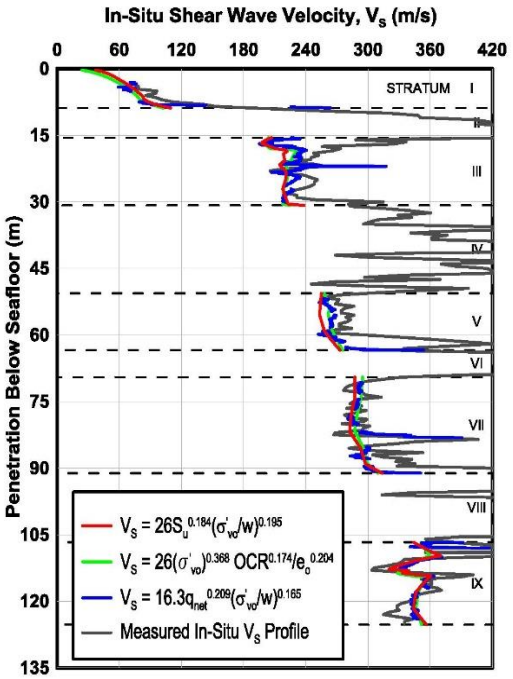

Figure 3. Comparison of V_S predicted with empirical correlations for clay and measured in situ V_S

Equations (2), (3), and (4) were applied to predict the in situ V_S at the 11 sites included in the database and 1 site not included in the database (Fig. 3). A comparison of the predicted in situ V_S values using these equations indicates that in general, the correlation that uses the undrained shear strength, equation (2), provides a lower bound of V_S; the relationship using the net cone resistance, equation (4), provides an upper bound of Vs; and the relationship that uses the effective vertical stress, OCR and void ratio, equation (3), provides an estimate closer to the upper bound generated by equation (4). This trend between predicted in situ V_S profiles using the above three equations is observed in figure 3.

G/G_{MAX}-γ AND D-γ CURVES OF BAY OF CAMPECHE CLAY

Two of the most important dynamic soil properties required to conduct an equivalent-linear seismic site response analysis to evaluate the soil amplification are: i) a curve of G/G_{max} versus cyclic shear strain γ, also called modulus reduction curve, where G is the shear modulus and G_{max} is the maximum shear modulus at very low shear strains of the order of 10^{-4} % and ii) a curve of equivalent hysteretic or material damping ratio D versus γ, where D is defined from the measured area (W_D) inside a complete hysteretic loop, which corresponds to the energy dissipated in one cycle, and the maximum strain energy stored during one cycle W_S, through the basic expression (see figure 4):

$$D = \frac{1}{2\pi}\frac{W_D}{G\gamma_c^2} = \frac{1}{4\pi}\frac{W_D}{W_S} \tag{5}$$

ISSN-e 2395-8251

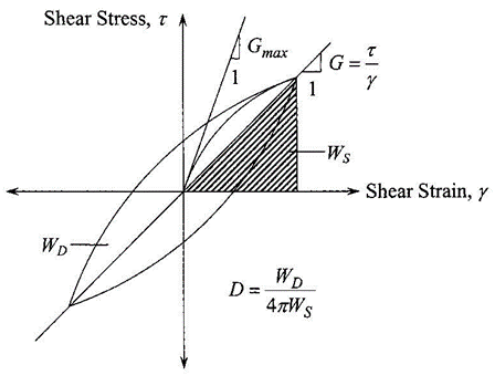

Figure 4. Hysteresis loop for one cycle of loading showing G_{max}, G, and D (Zhang, et al., 2005)

Typically, G/G_{max} decreases and D increases as γ becomes larger, and it has been observed that a fast decrease in G/G_{max} with γ, corresponding to a strongly nonlinear soil, is associated with a strong increase of D with γ in the same soil, and vice versa.

In general, G/G_{max} increase when the confining pressure (σ_m) increases. A simple way of explaining this trend is by focusing on the dependence of the shear modulus (G) on σ_m. The maximum shear modulus is defined as $G_{max} = A\ \sigma_m^m$, where m = 0.4 to 0.5 and A is a constant. For an isotropically consolidated sand, Coulomb's strength law indicates the shear strength (τ_{max}) increases linearly with σ_m ($\tau_{max} = \sigma_m \sin\phi$ for pure shear loading, where ϕ = angle of internal friction of the soil). Because $G = \tau/\gamma$ (figure 4), at large strains, $G = \tau_{max}/\gamma = \sigma_m \sin\phi /\gamma$; that is, G increases linearly with σ_m at large strains, whereas $G = G_{max}$ increases approximately with $\sigma_m^{0.5}$ at small strains. Therefore, G/G_{max} is proportional to $\sigma_m^{1-m} \approx \sigma_m^{0.5}$, and as σ_m increases, G/G_{max} increases. Conversely, the damping ratio (D) decreases.

It is generally difficult by any means to perform in situ tests in which large strains are imposed uniformly in the soil as it exists in the field. In realization of this, most recent efforts to pursue the strain dependency of modulus and damping of in situ soils have been directed toward the conduct of laboratory tests on undisturbed samples that are regarded as representing intact conditions in the field.

Unfortunately, it is not always possible to perform dynamic laboratory testing to obtain the shear modulus reduction curve and material damping ratio curve of all the soil strata found in the offshore soil deposit, and the geotechnical engineer is left to use curves developed mainly for onshore soils with different geological settings than those of the Bay of Campeche clay. Therefore, a characterization of the cyclic stress-strain response of the clay in shear that facilitates prediction of the shear modulus reduction curve and material damping ratio curve of clays of the Bay of Campeche is needed.

To cover this need, a database has been established and tailored for an equivalent linear characterization of the cyclic response of clay soil units in the Bay of Campeche. The data have been collected from offshore soil investigations performed between 2012 and 2015, which include abundant results of resonant column tests and cyclic DSS tests.

Summary of database of G/G_{max}–γ and D – γ of Bay of Campeche clay

The existing laboratory G/G_{max} and D data used in this study are compiled from offshore geotechnical investigations performed in the Bay of Campeche between 2012 and 2015 that include isotropically consolidated resonant column and strain-controlled cyclic DSS test results for 225 specimens of clay (Taboada, et al., 2017a).

ISSN-e 2395-8251

The Bay of Campeche clay database of 225 specimens is presented in figure 5a in terms of normalized shear modulus versus shear strain and is presented in figure 5b in terms of material damping ratio versus shear strain. The index properties for this database such as void ratio; overconsolidation ratio (OCR); carbonate content ($CaCO_3$); mean confining stress (σ'_m); and maximum shear modulus (G_{max}); and the range of values, average, and standard deviation for these index properties are presented in table 1.

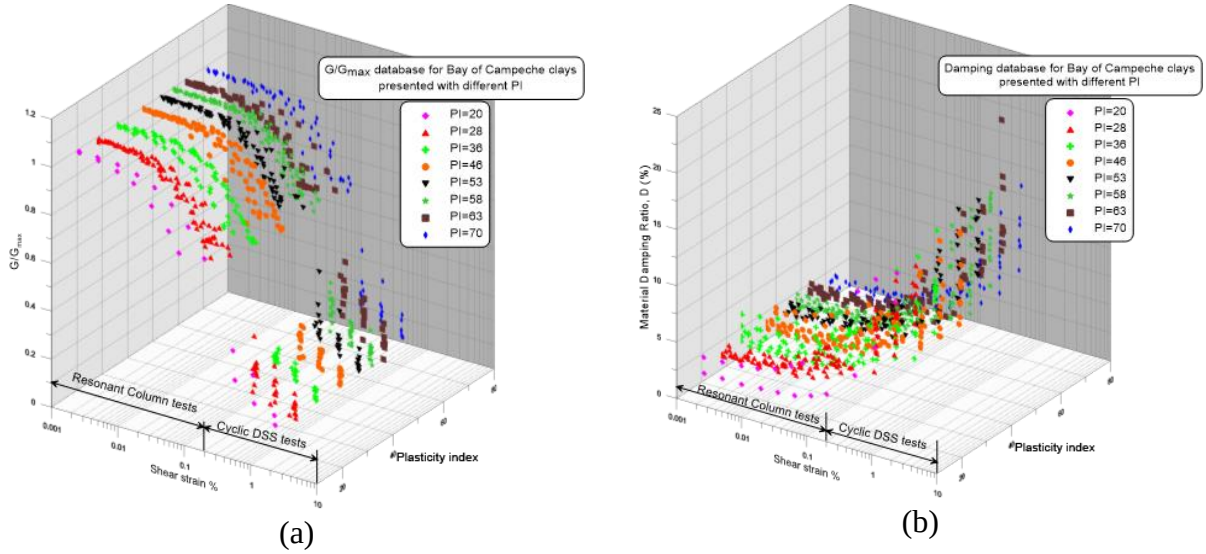

(a) (b)

Figure 5. G/G_{max}–γ and D – γ database of Bay of Campeche clay plotted with different plasticity index

Resonant column tests were performed on solid cylindrical clay specimens approximately 38 mm in diameter and 76 mm in length. Each test specimen was back-pressure saturated to about 140 kPa and then isotropically consolidated to 0.5, 1.0, and 2.0 times the in situ effective confining pressure.

Table 1. Index properties and its range of values, average, and standard deviation for the clay database

Index property	Range	Average	Standard deviation
e (-)	0.60-2.07	1.08	0.34
OCR (-)	1-10.5	2.8	1.9
$CaCO_3$ (%)	0-79	18.5	16.9
σ'_m (kPa)	30-875	365	274
PI (-)	17-74	49	14.1
G_{max} (MPa)	10-246	105	65.8

Strain-controlled cyclic DSS tests were conducted on clay specimens of approximately 18 mm to 19 mm in height, trimmed to approximately 67 mm in diameter. Each clay test specimen was consolidated to an effective vertical consolidation stress equal to the estimated in situ effective vertical stress. Each test specimen was consolidated to about one log cycle of time or 24 hours, whichever was less, past the end of primary consolidation (T_{100}) before applying 20 cycles of sinusoidal cyclic horizontal loads at a frequency of 1.0 Hz (for earthquake loading conditions). The test was conducted while maintaining the specimen at constant volume, with the pore pressures estimated by measuring the changes in the vertical stress during cycling. Each specimen was subjected to a specified nominal average cyclic shear strain of 0.25 %, 0.5 %, or 1.0 %.

ISSN-e 2395-8251

Modeling shear modulus degradation for clays

Darendeli (2001) proposed the following modified hyperbolic model based on testing on intact sand-gravel samples:

$$\left(\frac{G}{G_{max}}\right) = \frac{1}{1+\left(\gamma/\gamma_r\right)^{\alpha}} \tag{6}$$

where α is called the curvature parameter and γ_r is the reference strain value at which G/G_{max} = 0.5. This model uses only two parameters, and the reference strain provides an efficient normalization of shear strain.

Equation (6) is adopted to model the variation of G/G_{max} with γ of clay. Based on the database, the curvature parameter (α) is found to be influenced by the plasticity index (PI) of clay; the correlation is presented in equation (7). The reference strain (γ_r) is found to be a function of the normalized confining stress (σ'_m) with the atmospheric pressure (P_a) and PI of clay and is defined by equations (8) through (12).

$$\alpha = 0.0025 \times PI + 1.08 \tag{7}$$

$$\gamma_r = a \times \left(\frac{\sigma'_m}{P_a}\right)^k + c \tag{8}$$

$$k = 0.6903 \times e^{(-0.005 \times PI)} \tag{9}$$

$$c = 0.0006 \times e^{(0.072 \times PI)} \quad \text{if PI} \leq 45 \tag{10}$$

$$c = 0.0023 \times PI - 0.0827 \quad \text{if PI} > 45 \tag{11}$$

$$a = 0.065 \tag{12}$$

Figure 6a presents a comparison between measured and predicted G/G_{max} versus shear strain using equation (7) through equation (12) for the case of a clay with PI of 53 and varying σ'_m between 30 kPa and 800 kPa. Figure 6a demonstrates the predictions capture very well the measured values of G/G_{max} and for a given PI and G/G_{max} increases when σ'_m increases.

Figure 6b presents the effect of PI on G/G_{max} versus shear strain for a given confining stress of 400 kPa. The PI varies between 20 % and 70 %. Figure 6b demonstrates that at a given confining stress, G/G_{max} increases when the PI increases and the predicted values of G/G_{max} do not cover the whole range of measured values.

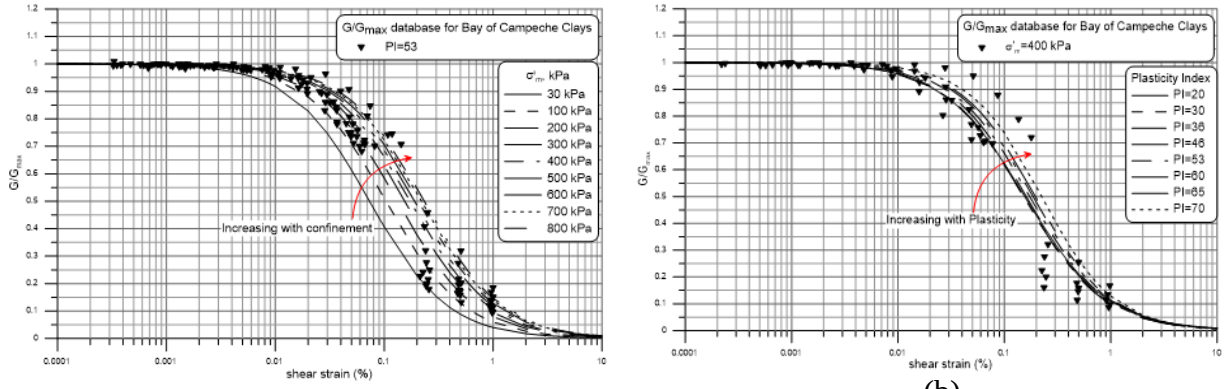

(a) (b)

Figure 6. Calculated $G/G_{max} - \gamma$ a) as function of σ'_m for PI=53 and b) as function of PI for σ'_m = 400 kPa

ISSN-e 2395-8251

Modeling material damping ratio versus cyclic shear strain (D-γ) for clays

The best-fit functional relationship adopted to model the variation of material damping ratio of clay versus cyclic shear strain is a modified hyperbolic equation similar to that proposed by Gonzalez and Romo (2011) in the form:

$$D = (D_{max} - D_{min}) \times \left[1 - \frac{1}{1+\left(\gamma/\gamma_{r_D}\right)^{\alpha_D}}\right] + D_{min} \quad (13)$$

where D_{max} and D_{min} are the maximum and minimum material damping ratios, respectively; γ_{rD} is the deformation corresponding to 50 % of increase in material damping ratio D (i.e., $D/D_{max} = 0.5$); and α_D is a curvature parameter characteristic of the curve D-γ.

A simple linear relation can be derived between (D_{max}-D_{min}), PI, and normalized effective confining pressure using all the available data, as:

$$D_{max} - D_{min} = (-0.008 * PI + 0.334) * \left(\frac{\sigma'_m}{P_a}\right) + 13.5 \quad (14)$$

The curvature parameter (α_D) is found to be a function of PI and defined by:

$$\alpha_D = 0.0025 \times PI + 1.08 \quad (15)$$

The Bay of Campeche clays of this database produce regression for the reference shear strain (γ_{rD}) as follows:

$$\gamma_{r_D} = a_D \times \left(\frac{\sigma'_m}{P_a}\right)^{k_D} + c_D \quad (16)$$

$$k_D = 1.14 \times e^{(0.0013 \times PI)} \quad (17)$$

$$c_D = 0.0027 \times PI - 0.0609 \quad (18)$$

$$a_D = 0.08 \quad (19)$$

The trend of minimum material damping ratio (D_{min}) with normalized effective confining pressure σ'_m, with the atmospheric pressure (P_a) can be presented in a form as shown below:

$$D_{min} = (-0.246) \times \left(\frac{\sigma'_m}{p_a}\right) + 2.75 \quad (20)$$

Figure 7a presents a comparison between measured and the predicted damping ratio (D) versus shear strain using equation (13) and equations (14) through (20) for the case of a clay with plasticity index of 53 and varying confining pressure between 30 kPa and 800 kPa. Figure 7a demonstrates the predictive curves of D - γ fit very well the range of measured values of damping ratio. It also is observed that for a given PI, the damping ratio decreases as the confining pressure increases.

Figure 7b presents the effect of PI on D versus shear strain for a given confining stress of 400 kPa. The PI varies between 20 % and 70 %. Figure 7b demonstrates that at a given confining stress, D decreases when PI increases, and the predicted values of D cover most of measured values.

Validation of proposed model for clays

In the case of unavailability of the shear modulus degradation curve for clays, it is possible to calculate it with equation (6) and equations (7) to (12). Comparison between measured and predicted values can be validated against the database. The comparison between 787 measured and calculated values of G/G_{max} presented in figure 8a illustrates that there is an excellent agreement between measured and calculated values for $G/G_{max} > 0.6$ corresponding to the low strain range of the resonant column data. However, the agreement deteriorates falling outside the factor of 1.3 and 0.7 from the measurements in the range of $0.4 > G/G_{max} > 0.2$, and the measurements are underpredicted when $0.2 > G/G_{max}$.

In the absence of site-specific data on the material damping ratio (D) versus shear strain for clays from the Bay of Campeche, it is possible to calculate them with equation (13) and equations (14) to (20). The comparison between 787 damping ratio measurements and predicted values presented in figure 8b shows most of the calculated values of damping ratio in the range of $16 > D > 4$ fall within a factor of 1.3 and 0.7 from the measurements, indicating very good agreement with the cyclic DSS test data at strains larger than 0.1 %. Some of the calculated values of damping ratio underpredict the measurements when 4 % > D, corresponding to small shear strains of the resonant column test data.

ISSN-e 2395-8251

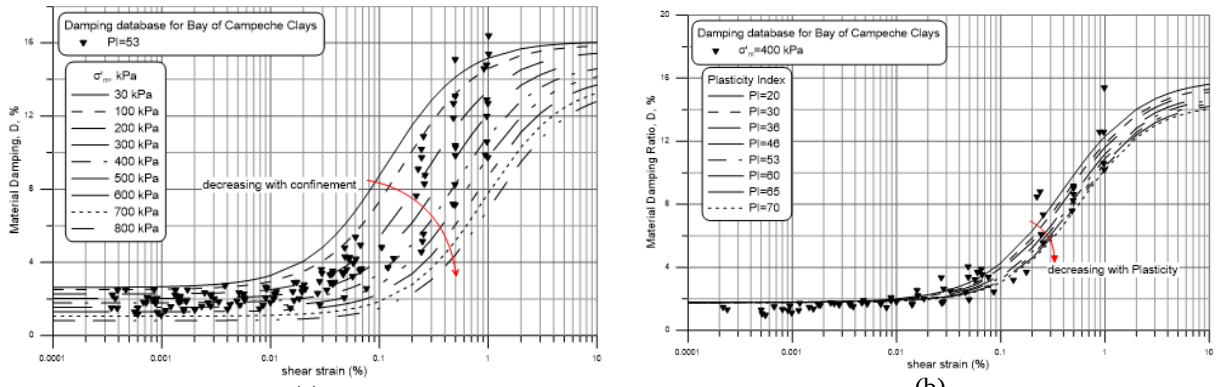

(a) (b)

Figure 7. Calculated D – γ a) as function of σ'$_m$ for PI=53 and b) as function of PI for σ'$_m$ = 400 kPa

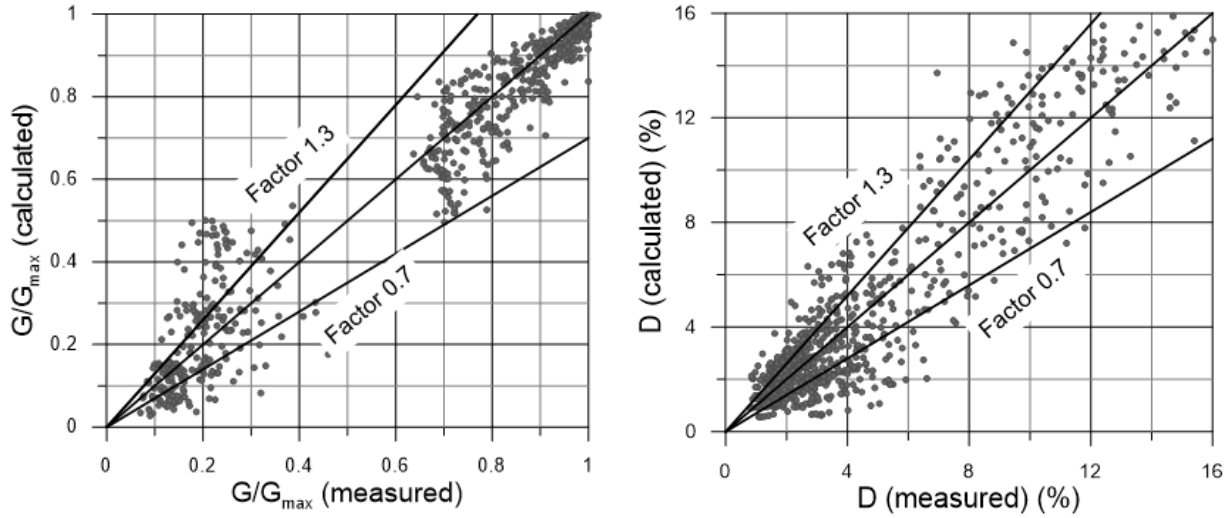

(a) (b)

Figure 8. Comparison of 787 measured and calculated values of a) G/G$_{max}$ and b) damping ratio D

Comparison with previously published models for clays

The calculated G/G$_{max}$ and D and those of Darendeli (2001), Vucetic and Dobry (1991), and Gonzalez and Romo (2011) for σ'$_m$ of 400 kPa and plasticity index (PI) of 50 are shown in figure 9. The recommended G/G$_{max}$ curve for Bay of Campeche clay is similar to Vucetic and Dobry (1991) for shear strains up to 0.08 % and it follows closely the Darendeli (2001) curve for strains larger than 0.3%. The G/G$_{max}$ curve of Gonzalez and Romo (2011) for shear strain smaller than 1 % falls outside the range defined by the rest of shear modulus curves presented in figure 9a. The shear modulus curve of the Bay of Campeche clay falls within the range defined by Darendeli (2001) and Vucetic and Dobry (1991) curves.

The recommended damping ratio curve for the Bay of Campeche clay for σ'$_m$ of 400 kPa and plasticity index (PI) of 50 shown in figure 9b is very similar to Gonzalez and Romo (2011) curve, is below the Vucetic and Dobry (1991) curve, and has large discrepancies with the damping ratio curve of Darendeli (2001).

The discrepancies in damping ratio between the damping ratio curve developed in the present study for the Bay of Campeche clay and Darendeli (2001) curve can produce large differences when they are used to perform earthquake response analyses, as observed by Taboada, et al., (2017b) giving lower amplification of accelerations that are unconservative for the case when the Darendeli (2011) damping curve is utilized.

ISSN-e 2395-8251

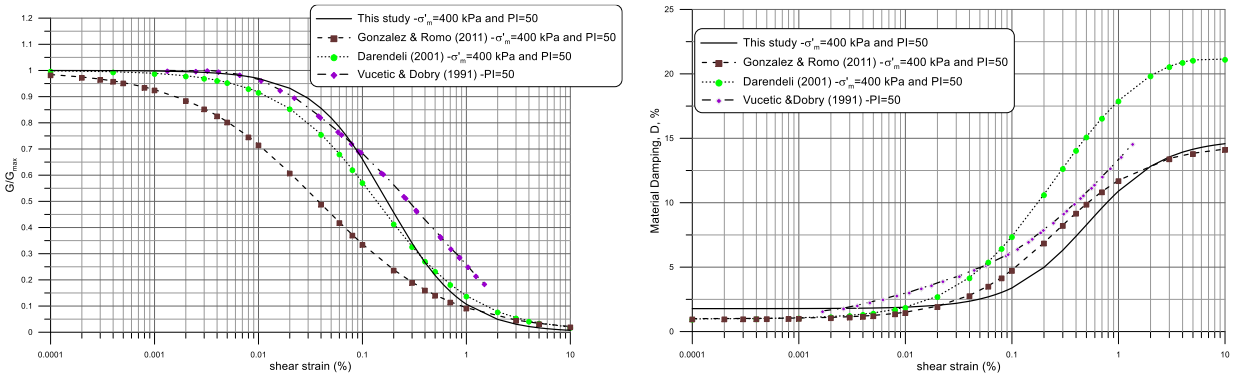

(a) (b)

Figure 9. Comparison of calculated curves for σ'_m = 400 kPa and PI = 50 for the Bay of Campeche clay with Vucetic and Dobry (1991), Darendeli (2001), and Gonzalez and Romo (2011) for a) $G/G_{max} - \gamma$ and b) D-γ

G/G$_{MAX}$-γ AND D-γ OF BAY OF CAMPECHE CALCAREOUS CLAY TO CARBONATE MUD

Summary of database of G/G$_{max}$-γ and D-γ of calcareous clay to carbonate mud

ISSN-e 2395-8251

The database of G/G_{max} and D curves used in this study was developed based on clays with carbonate content higher than 10 % retrieved from the Bay of Campeche and Tabasco Coastline during geotechnical campaigns performed between 1993 and 2015 (Cruz, et al., 2015). The database contains test results of isotropically consolidated resonant column and strain-controlled cyclic DSS tests. The number of cycles of loading (N) of the cyclic DSS data is 15.

Figure 10a shows the database of modulus reduction curves G/G_{max} versus cyclic shear strain of the Bay of Campeche and Tabasco Coastline clays with carbonate content between 10 % and 50 %, 50 % and 90 %, and 90 % and 100 %. Figure 10b shows the database of material damping ratio curves versus cyclic shear strain of the Bay of Campeche and Tabasco Coastline clays with carbonate content between 10 % and 50 %, 50 % and 90%, and 90 % and 100 %. This database of modulus reduction curves and material damping ratio curves contain the results of 252 dynamic test.

Figure 11 shows histograms of depth, liquid limit (LL), plasticity index (PI), carbonate content ($CaCO_3$), overconsolidation ratio (OCR), and mean effective confining pressure (σ'_m) of all the soil specimens of the database of clays with carbonate content between 10 % and 100 %.

The range of values, average, and standard deviation of the index properties of the database, including depth, OCR, LL, plastic limit (PL), PI, σ'_m, and carbonate content ($CaCO_3$), are presented in table 2.

The plasticity index chart of the database contains a total of 160 points and is presented in figure 12.

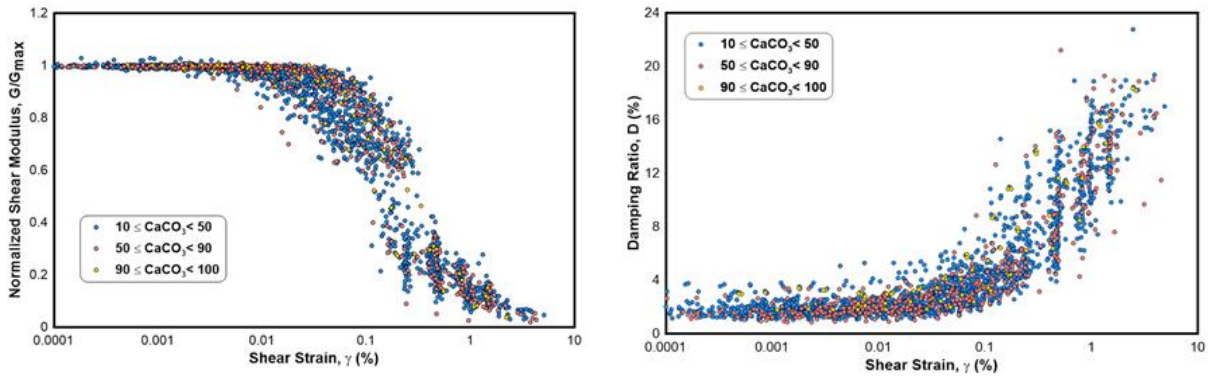

(a) (b)

Figure 10. Calcareous clay, clayey carbonate mud, and carbonate mud database of a) G/G_{max}-γ and b) D-γ

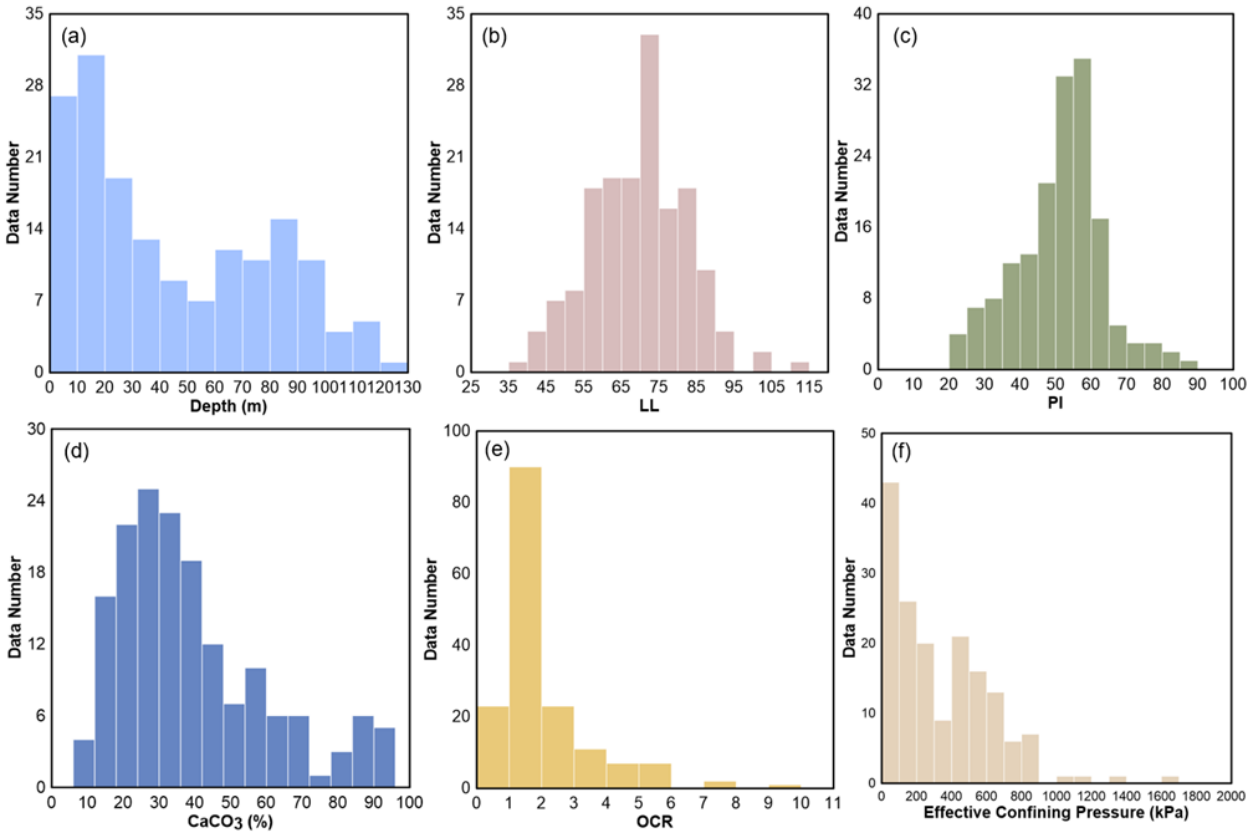

Figure 11. Histograms of depth, LL, PI, $CaCO_3$, OCR, and σ'_m of the database of calcareous clay to carbonate mud

Table 2. Index properties of database, its range of values, average, and standard deviation

Index Property	Range	Average	Standard Deviation
Depth (m)	3 - 125	45	34
OCR	1.0 - 10.5	2.3	1.5
LL	39 - 112	70	13
PL	4- 45	20	7
PI	21 - 88	51	12
σ'_m (kPa)	20 - 1670	336	285
$CaCO_3$ (%)	10 - 94	40	21

ISSN-e 2395-8251

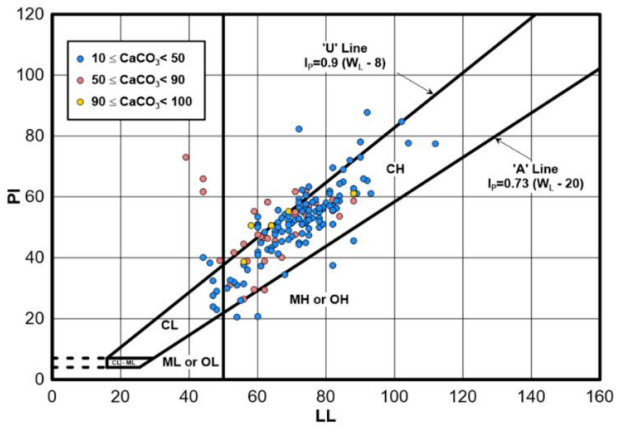

Figure 12. Plasticity index chart of the database of calcareous clays, clayey carbonate mud, and carbonate mud

Modeling shear modulus reduction curve G/G_{max}-γ of calcareous clay to carbonate mud

Equation (6) is adopted in this study to model the variation of G/G_{max} with γ. Based on the database, the curvature parameter (α) is influenced by the PI of clay (Taboada, et al., 2021), and the correlation is presented in equation (21).

$$\alpha = E_G \times PI + F_G \tag{21}$$

The reference strain (γ_r) is found to be a function of mean effective confining stress (σ'_m) and PI of clay, and it is defined by equations (22) through (24). P_a is the atmospheric pressure in the same units of σ'_m.

$$\gamma_r = A_G \times \left(\frac{\sigma'_m}{P_a}\right)^{K_G} + C_G \tag{22}$$

$$K_G = B_G \times e^{D_G \times PI} \tag{23}$$

$$C_G = M_G \times PI + N_G \tag{24}$$

where E_G, F_G, A_G, B_G, D_G, M_G, and N_G are fitting parameters given in table 3 to model the shear modulus reduction curve (G/G_{max}–γ) of calcareous clay ($10\,\% \leq CaCO_3 < 50\,\%$) and clayey carbonate mud ($50\,\% \leq CaCO_3 < 90\,\%$).

Table 3. Fitting parameters for modeling shear modulus degradation curves G/G_{max}-γ

Carbonate Contents (%)	A_G	B_G	D_G	M_G	N_G	E_G	F_G
10 – 50	0.085	0.75	−0.008	0.0030	−0.055	0.0066	1.0570
50 – 90	0.040	0.95	−0.006	0.0048	−0.130	0.0115	0.8783

Figure 13a shows the effect of carbonate content ($CaCO_3$) and mean effective confining stress (σ'_m) in the modulus reduction curve (G/G_{max}-γ) considering the case of calcareous clay and clayey carbonate mud with a PI = 50 and for σ'_m varying between 10 kPa and 1400 kPa based on equation (6), equations (21) through (24), and the fitting parameters reported in table 3. The computed curves in this figure show that as $CaCO_3$ increases, the G/G_{max} curve tends to shift downward (if a given value of γ, $CaCO_3$ increases, G/G_{max} is reduced). This figure also shows that as σ'_m increases, the G/G_{max} curve tends to shift upward (if a given value of γ, σ'_m increases, G/G_{max} rises).

ISSN-e 2395-8251

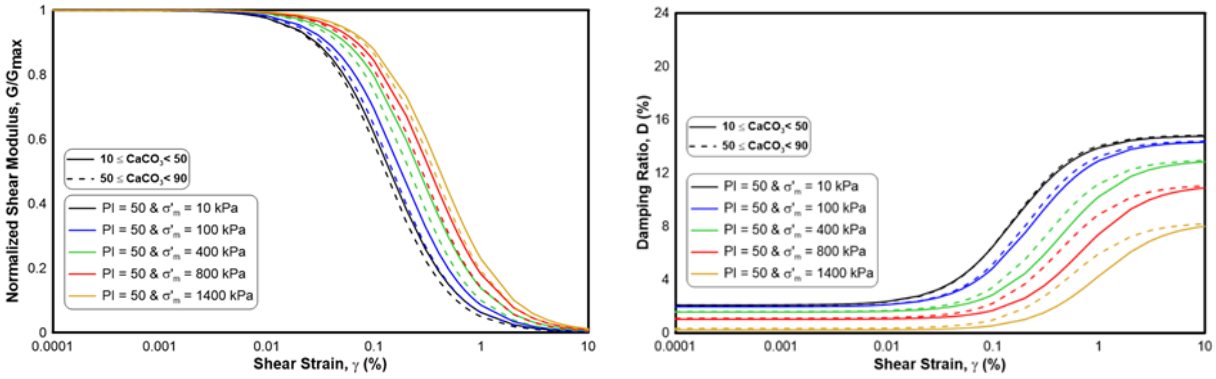

(a) (b)

Figure 13. Effect of $CaCO_3$ and σ'_m in normalized shear modulus G/G_{max}-γ and material damping D-γ curves

Modeling material damping ratio curve D-γ for calcareous clay and clayey carbonate mud

Equation (13) was used to model the material damping ratio curve of clays with carbonate content between 10 % and 90 % where a simple linear relation can be derived between ($D_{max} - D_{min}$), plasticity index, and normalized effective confining pressure using all the available data, as:

$$D_{max} - D_{min} = (U_D * PI + V_D) * \left(\frac{\sigma'_m}{P_a}\right) + W_D \quad (25)$$

The curvature parameter (α_D) is found to be a function of plasticity index (PI) and defined by:

$$\alpha_D = E_D \times PI + F_D \quad (26)$$

The Bay of Campeche clays with carbonate content between 10 % and 100 % of this database produce regression for the reference shear strain (γ_{rD}) as follows:

$$\gamma_{r_D} = A_D * \left(\frac{\sigma'_m}{P_a}\right)^{K_D} + C_D \quad (27)$$

$$K_D = B_D \times e^{H_D \times PI} \quad (28)$$

$$C_D = M_D \times PI + N_D \quad (29)$$

The trend of minimum material damping ratio (D_{min}) with normalized effective confining pressure can be presented in the form shown below:

$$D_{min} = O_D * \left(\frac{\sigma'_m}{P_a}\right) + Q_D \quad (30)$$

where U_D, V_D, W_D, E_D, F_D, A_D, B_D, H_D, M_D, N_D, O_D, and Q_D are fitting parameters given in table 4 to model the damping ratio curve (D-γ) of calcareous clay ($10\ \% \leq CaCO_3 < 50\ \%$) and clayey carbonate mud ($50\ \% \leq CaCO_3 < 90\ \%$).

ISSN-e 2395-8251

Table 4. Fitting parameters for modeling material damping ratio curves

Carbonate content (%)	A_D	B_D	H_D	M_D	N_D	E_D	F_D	U_D	V_D	W_D	O_D	Q_D
10 – 50	0.09	0.9	−0.001	0.0045	−0.08	0.0066	1.0570	−0.0043	−0.1247	12.75	−0.136	2.109
50 – 90	0.07	1.0	−0.008	0.0040	−0.06	0.0090	0.9894	−0.0041	−0.1474	12.79	−0.128	2.118

Figure 13b shows the effect of carbonate content ($CaCO_3$) and mean effective confining stress (σ'_m) on the material damping ratio curve (D-γ) considering the case of calcareous clay and clayey carbonate mud with a PI = 50 and for σ'_m varying between 10 kPa and 1400 kPa based on equation (13), equations (25) through (30), and the fitting parameters reported in table 4. The computed curves in this figure show that as $CaCO_3$ increases, the D curve tends to shift upward (if a given value of γ, $CaCO_3$ increases, D rises). This figure also shows that as σ'_m increases the damping ratio curve D-γ tends to shift downwards (if a given value of γ, σ'_m increases, D is reduced).

Validation of G/G_{max}-γ and D-γ curves of calcareous clay and clayey carbonate mud

The validation of the calculated G/G_{max}-γ and D-γ curves can be best assessed by plotting them against the 3217 G/G_{max} data points measured in the dynamic laboratory tests (2553 data point for calcareous clay and 664 data points for clayey carbonate mud). Figure 14a presents the measured versus calculated G/G_{max} values of calcareous clay and clayey carbonate and shows the accuracy of G/G_{max} (calculated) increases as G/G_{max} (measured) increases. The prediction is very good for G/G_{max} (measured) values between 0.6 and 1.0, with most of G/G_{max} (calculated) falling within a factor of 1.25 and 0.75 of G/G_{max} (measured). In the range of G/G_{max} (measured) between 0.2 and 0.6, most of the G/G_{max} (calculated) values fall within a factor of 0.5 and 1.5 of G/G_{max} (measured). Finally, for G/G_{max} (measured) smaller than 0.2, G/G_{max} (calculated) are most of the time underestimating G/G_{max} (measured) by as much as 50 %. This underprediction corresponding to cyclic shear strains in the range of 1% and 10% is a limitation of the proposed model where all the calculated modulus reduction curves converge at a value G/G_{max} of about zero when γ = 10 %, as shown in figure 14a.

Figure 14b shows D (measured) versus D (calculated) of calcareous clay and clayey carbonate mud and shows that the accuracy of D (calculated) increases as D (measured) increases. For D (measured) > 6 %, most of the material damping ratio D (calculated) falls within a factor of 1.25.and 0.75 of D (measured), indicating a very good prediction of material damping ratio at cyclic shear strains larger than 0.10 %. In the range of D (measured) < 6 %, the prediction deteriorates and some of the D (calculated) values fall outside a factor of 1.5 and 0.5 of D (measured), indicating that in this range corresponding to cyclic shear strains smaller than 0.1 % D (calculated) can overpredict up to 50 % the D (measured) values or underpredict up to 50 %. This is a model limitation at small cyclic shear strains where the model predicts a wide range of damping ratios, as observed in figure 13b.

Comparison with published G/Gmax-γ and D-γ curves of clays without carbonate content

The calculated modulus reduction curves G/G_{max}-γ presented in figure 13a of calcareous clay and clayey carbonate mud with σ'_m = 400 kPa and plasticity index PI = 50 are compared with previously published modulus reduction curves of non-calcareous clays developed for the corresponding mean effective confining pressure and plasticity index by Vucetic and Dobry (1991), Darendeli (2001), Gonzalez and Romo (2011), and Taboada, et al. (2017a).

ISSN-e 2395-8251

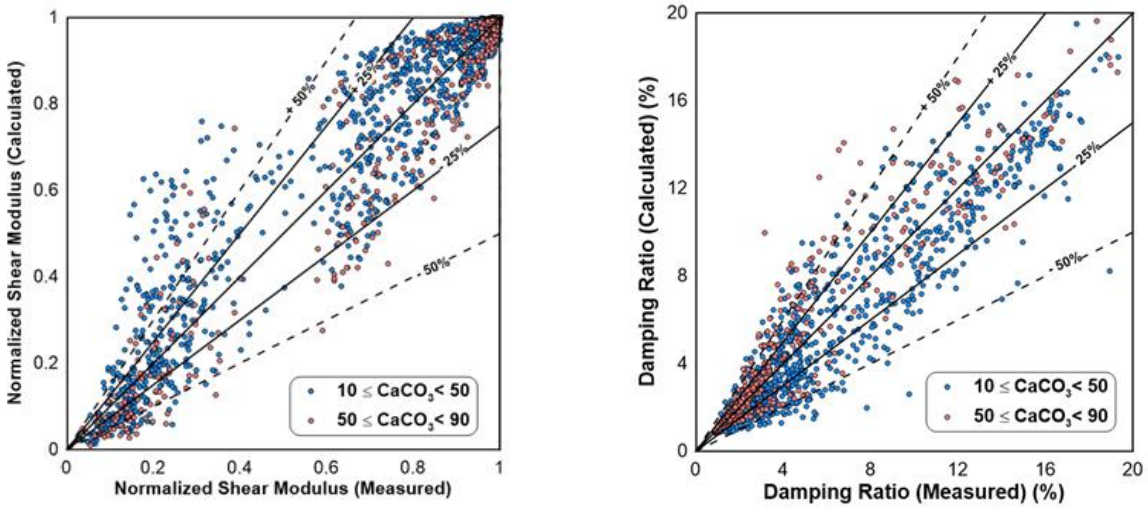

(a) (b)

Figure 14. Comparison of measured and calculated G/G_{max} and D values considering a total of 3217 measured points

Figure 15a shows that the calculated curves G/G_{max}-γ of calcareous clay and clayey carbonate mud are more linear with a higher threshold cyclic shear strain than the curve of Taboada, et al. (2017a). After the threshold strain is reached, the calculated curves degrade at a slightly higher rate than the curve of Taboada, et al., (2017a) and meet at a cyclic strain of 2 %, and after that they overlap and become only one curve.

Figure 15a shows that the calculated G/G_{max}-γ curves of calcareous clay and clayey carbonate mud are more linear and have a higher threshold shear strain than the corresponding curve of Darendeli (2001) of non-calcareous clay. After the threshold strain is reached, the calculated modulus reduction curves degrade at a higher rate, cross, and remain slightly below the curve of Darendeli (2001) at cyclic shear strains larger than 1 %.

Figure 15a shows that the calculated G/G_{max}-γ curves of calcareous clay and clayey carbonate mud are more linear, have a higher threshold shear strain than the modulus reduction curve for a plasticity index of 50 of Vucetic and Dobry (1991). After the threshold strain is reached, the calculated modulus reduction curves degrade at a higher rate, cross at a cyclic shear strain of 0.6 %, and fall below the Vucetic and Dobry (1991) curve at higher strains.

Figure 15a shows that the calculated G/G_{max}-γ curves of calcareous clay to carbonate mud are significantly more linear with a threshold shear strain considerably higher than the curve of Gonzalez and Romo (2011). After the threshold strain is reached, the shear modulus degrades at a much higher rate until they meet at a cyclic shear strain of 2 %, after which they continue slightly lower than the curve of Gonzalez and Romo (2011).

After comparison with four modulus reduction curves of clay found in the literature, the calculated G/G_{max}-γ curves of calcareous clay and clayey carbonate mud show the most linear response, having the highest threshold shear strain. After the threshold strain is reached, the calculated modulus reduction curves degrade at the highest rate, meet all the non-calcareous curves at a cyclic shear strain of 1 % (except Vucetic and Dobry (1991)), and almost overlap.

ISSN-e 2395-8251

Figure 15b shows the material damping ratio curves of calcareous clay and clayey carbonate mud for σ'_m of 400 kPa and PI of 50 and compares them with previously published D-γ curves of non-calcareous clays developed for the corresponding mean effective confining pressure and PI by Vucetic and Dobry (1991), Darendeli (2001), Gonzalez and Romo (2011), and Taboada, et al. (2017a).

The calculated D-γ curves developed for calcareous clay and clayey carbonate mud dissipate slightly more energy than the corresponding curve of Taboada, et al. (2017a). They intersect at a cyclic shear strain of about γ = 1.5 %, and beyond this γ, the calculated D-γ curves dissipate less energy than the curves of Taboada, et al. (2017a).

The calculated D-γ curves developed for calcareous clay and clayey carbonate mud dissipate more energy than the corresponding curve of Gonzalez and Romo (2011) for cyclic shear strains smaller than 0.02 %. For cyclic shear strains larger than 0.02 %, the calculated curves dissipate less energy than the curve of Gonzalez and Romo (2011).

The calculated D-γ curves developed for calcareous clay and clayey carbonate mud dissipate the same amount of energy as the corresponding curve of Vucetic and Dobry (1991) for cyclic shear strains smaller than 0.002 %. For cyclic shear strains higher than 0.002 %, the curve of Vucetic and Dobry (1991) dissipates more energy than the calculated curves, but the difference in damping is not very large.

The calculated D-γ curves developed for calcareous clay and clayey carbonate mud differ considerably from the curve of Darendeli (2001), dissipating considerably less energy for cyclic shear strains larger than 0.01 %.

ISSN-e 2395-8251

The large discrepancies in material damping ratio curves found between the curves developed in the present study and Darendeli (2001) can produce large differences when they are used to perform site response analyses, as observed by Taboada, et al., (2017b), giving lower amplification of accelerations that are unconservative for the case when the Darendeli (2011) damping curve is utilized.

After comparison with four material damping curves of non-calcareous clay found in the literature, the calculated D-γ curves of calcareous clay and clayey carbonate mud display the lowest material damping ratio over the range of 0.01 < γ < 10 %. At cyclic shear strains smaller than about 0.01 %, the curves of Gonzales and Romo (2011) and Darendeli (2001) show the lowest damping ratio.

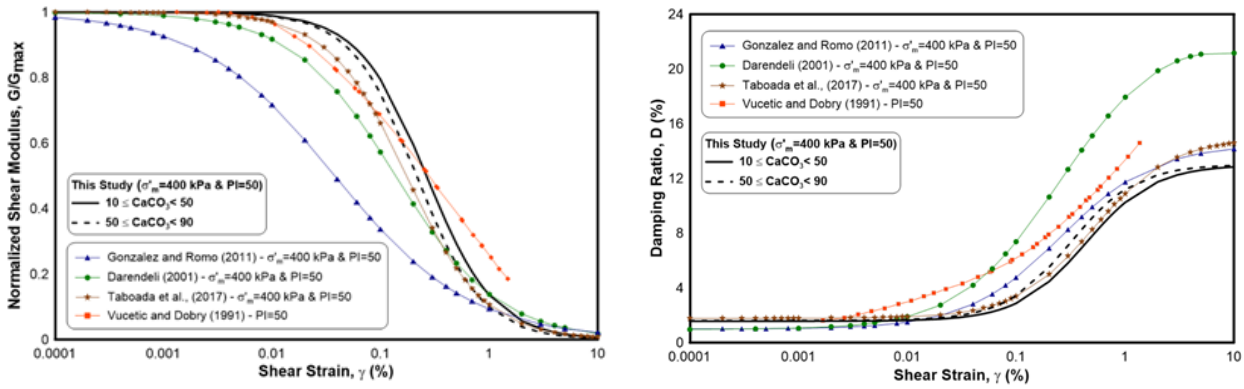

(a) (b)

Figure 15. Comparison of G/G_{max} -γ and D-γ curves of calcareous clay and clayey carbonate mud with clays

CONCLUSIONS AND RECOMMENDATIONS

A database of in situ V_S measurements with a P-S suspension seismic velocity logger and standard geotechnical engineering material properties for the Bay of Campeche clays has been established. The database allowed the development of several empirical correlations between in situ V_S, basic soil properties of clay, and cone net resistance. These equations should be used with caution in predicting the in situ shear wave velocity in the top 3.5 m because there were no V_S measurements in these surficial soils due to the noise transmitted from the vessel to the time records used for V_S determination, which made shear wave arrivals difficult to pick. It is recommended the predictions of V_S made with the relationships in the top 3.5 m should be limited to a lowest value of 35 m/s.

The following 3-step procedure is recommended to determine the three Vs profile of clay and sand needed to perform earthquake response analysis in the Bay of Campeche when in situ measurements of V_S at the site are not available:

- First, develop the best estimate in situ V_S profile in clay by calculating the average of the three V_S values estimated using equations (2), (3), and (4).
- Second, develop the best estimate in situ V_S profile in sand by calculating the average of the three V_S values estimated using equations (12), (14), and (16) presented in Taboada, et al., (2015).
- Third, to incorporate the potential for variation in the site conditions and the uncertainties in the best estimate in situ shear wave velocity three different shear wave velocity profiles must be analyzed for each acceleration time history: the best estimate V_S, a lower V_S case, and a higher V_S case. The lower and higher V_S cases are estimated by applying scaling factors of $(2/3)^{1/2} = 0.816$ and $(3/2)^{1/2} = 1.225$ to the best estimate in situ shear wave profiles obtained in the previous two steps. These scaling factors are recommended in ASCE 4-98 (1998).

ISSN-e 2395-8251

A database of resonant column and strain-controlled cyclic DSS tests was developed for the following soil types: clay, calcareous clay and clayey carbonate mud. The database allowed the development of predicting equations based on two independent modified hyperbolic relationships to determine the normalized shear modulus G/G_{max}-γ and material damping ratio D-γ curves when no dynamic test results are available for a given soil layer within the strata.

The predictive equation of G/G_{max} in the form of equation (6) features two curve-fitting parameters: reference strain γ_r at $G/G_{max} = 0.5$ and a curvature parameter α. For simplicity, the curvature parameter α was given a linear relationship with plasticity index. An exponential relation between the reference strain γ_r and the normalized effective confining stress with respect to the atmospheric pressure, σ'_m/P_a, was established for the most common range of effective confining stresses ($\sigma'_m = 50$ kPa – 1,200 kPa).

The predictive equation of material damping ratio in the form of equation (13) features four curve-fitting parameters: reference strain γ_{rD} at $D/D_{max} = 0.5$; a curvature parameter α_D characteristic of the curve D-γ; and maximum and minimum material damping ratios, D_{max} and D_{min}, respectively. For simplicity, the curvature parameter α_D was given a linear relationship with plasticity index. An exponential relation between the reference strain γ_{rD} and the normalized effective confining stress with respect to the atmospheric pressure, σ'_m/P_a, was established. A linear relation was established between σ'_m/P_a, and D_{min}. A linear relation between $(D_{max} - D_{min})$ and σ'_m/P_a was established.

It is shown that as $CaCO_3$ increases, the G/G_{max} curve tends to shift downward, and the damping ratio curve tends to shift upward and the influence in the shape of the G/G_{max} is evident when the carbonate content is higher than 50 % and more pronounced in sand than in clay. As σ'_m and PI increase, the G/G_{max}

curve tends to shift upward and the damping ratio curve tends to shift downward, and the value of OCR has practically no effect on the position of the curves. The effect of σ'_m was more important than the PI as opposed to the findings of Vucetic and Dobry (1991), where the position of the curves was not affected by σ'_m and PI was the most important property in defining the position of the curves.

The validation of the calculated values of G/G_{max} and D shows the best predictions are found at low shear strains for G/G_{max} and at large shear strains for D falling within $\pm$ 25 % of the measured values. Due to the limitations in the model at large strains ($\gamma > 1$ %) for G/G_{max} and at low strains ($\gamma < 0.05$ %) for D, the calculated values fall within $\pm$ 50 % of the measured values.

Comparisons between the predictive equations developed in this study and the earlier previously published curves show the predictive equations of this study of G/G_{max} exhibits the most linear response and the largest threshold shear strain, and beyond the threshold strain the curve degrades at the highest rate. The predictive equations of material damping ratio provide the lowest material damping ratio for cyclic shear strains larger than 0.01 %.

The equations developed to calculate V_S, and the curves of G/G_{max}-γ and D-γ of Bay of Campeche clays are recommended for preliminary or perhaps even final seismic site response evaluations. It has been shown that they can be used in practice to perform earthquake response analysis in the Bay of Campeche and determine the design acceleration spectrum at the depth of maximum soil-pile interaction (Taboada, et al., 2017b; Taboada, et al., 2022).

However, considering the scatter of the data points around V_S and the curves, the equations should be used with caution, and parametric and sensitivity studies are strongly recommended to assess the importance of this scatter. In large critical projects, in situ measurements of V_S and direct experimental determinations of G/G_{max} and D for the soils of interest are suggested to be more appropriate.

ISSN-e 2395-8251

ACKNOWLEDGEMENTS

This research was made possible thanks to the work performed offshore by roughnecks, drillers, engineers, laboratory technicians, and marine crew to collect high-quality soil samples in the Bay of Campeche; the onshore dynamic laboratory testing performed by the laboratory technicians at Fugro's Houston laboratory; and the quality assurance and quality control of the test results performed by onshore engineers in Houston. Their dedication and skills are greatly appreciated.

REFERENCES

American Society of Civil Engineers, ASCE 4-98 (1998). *Seismic analysis of safety-related nuclear structures and commentary*. American Society of Civil Engineers. https://doi.org/10.1061/9780784404331

Cruz, D, M Lopez, F A Flores, P Barrera, E Rojas, R Torres, M Cervantes, J M Hernández, & S Renovato (2015). "System information of geophysical and geotechnical data of marine soils of the Gulf of Mexico". *Proceedings of the XV Panamerican Conference of Soil Mechanics and Geotechnical Engineering, Buenos Aires, Argentina, November*.

Darendeli, B M (2001). "Development of a new family of normalized modulus reduction and material damping curves". *Doctoral dissertation*, University of Texas.

Gonzalez, C M, & M P Romo, (2011). "Estimación de propiedades dinámicas de arcillas". *Revista de Ingenieria Sismica*, *84*, 1–23. http://dx.doi.org/10.18867/RIS.84.19

Taboada, V M, D Cruz, P Barrera, E Espinosa, D Carrasco & K C Gan (2013). "Predictive equations of shear wave velocity for Bay of Campeche clay". *Proceedings of the 45th Offshore Technology Conference*. http://dx.doi.org/10.4043/24068-MS

Taboada, V M, D Cruz, P Barrera, S D Renovato, J M Hernández & K C Gan (2015). "Predictive equations of shear wave velocity for Bay of Campeche Sand". *Proceedings of the third International Symposium on Frontiers in Offshore Geotechnics III* (pp. 1115–1120). Taylor & Francis Group.

Taboada, V M, V Dantal, D Cruz, F A Flores, R E Vazquez, & P Barrera (2017a). "Normalized modulus reduction and material damping ratio curves for Bay of Campeche clay". *Proceedings of the 8th International Conference Offshore Site Investigation and Geotechnics (OSIG), Volume 1*. Society for Underwater Technology (SUT).

Taboada, V M, F A Flores, V Dantal, D CruZ & P Barrera (2017b). "Seismic site response analyses of Bay of Campeche Clay using predicted dynamic soil properties". *Offshore Technology Conference*. http://dx.doi.org/10.4043/27541-MS.

Taboada, V M, S C Cao, F A Flores, D Cruz & P Barrera (2021). "Normalized Modulus Reduction and Damping Ratio Curves for Bay of Campeche calcareous clay to carbonate mud". *Offshore Technology Conference*. http://dx.doi.org/10.4043/31153-MS.

Taboada, V M, S H Cao, D Cruz, P Barrera & F A Flores (2022). "Using predicted Dynamic properties to perform seismic site response analyses on a Bay of Campeche calcareous soil deposit". *Offshore Technology Conference*. http://dx.doi.org/31809-MS.

Vucetic, M & R Dobry (1991). "Effect of soil plasticity on cyclic response". *Journal of Geotechnical Engineering*, *117*(1), 89–107. https://doi.org/10.1061/(ASCE)0733-9410(1991)117:1(89)

Zhang, J, R D Andrus, & C Hsein Juang (2005). "Normalized shear modulus and material damping ratio relationships". *Journal of Geotechnical and Geoenvironmental Engineering, ASCE*, *131*(4). https://doi.org/10.1061/(ASCE)1090-0241(2005)131:4(453)

ISSN-e 2395-8251